How to extract adsorption energies, adsorbate-adsorbate interaction parameters and saturation coverages from temperature programmed desorption experiments

Vijay, Sudarshan; Kristoffersen, Henrik H.; Katayama, Yu; Shao-Horn, Yang; Chorkendorff, Ib; Seger, Brian; Chan, Karen

Published in:
Physical Chemistry Chemical Physics

Link to article, DOI:
10.1039/d1cp01992a

Publication date:
2021

Document Version
Early version, also known as pre-print

How to extract adsorption energies, adsorbate-adsorbate interaction parameters, and saturation coverages from temperature programmed desorption experiments

*Sudarshan Vijay[1], Henrik H. Kristoffersen[1], Yu Katayama[3,4], Yang Shao Horn[3,5,6], Ib Chorkendorff[2] , Brian Seger[2], Karen Chan[1]**

AUTHOR ADDRESS

1. *CatTheory, Department of Physics, Technical University of Denmark, 2800 Kgs. Lyngby, Denmark*
2. *SurfCat, Department of Physics, Technical University of Denmark, 2800 Kgs. Lyngby, Denmark*
3. *Research Laboratory of Electronics, Massachusetts Institute of Technology, Cambridge, MA 02139, USA*
4. *Department of Applied Chemistry, Graduate School of Sciences and Technology for Innovation, Yamaguchi University, Tokiwadai, Ube, 755-8611, Japan*

5. *Department of Mechanical Engineering, Massachusetts Institute of Technology, Cambridge, MA 02139, USA*

6. *Department of Materials Science and Engineering, Massachusetts Institute of Technology, Cambridge, MA 02139, USA*

AUTHOR INFORMATION

Corresponding Authors*

kchan@fysik.dtu.dk

ABSTRACT

We present a simple scheme to extract the adsorption energy, adsorbate interaction parameter and the saturation coverage from temperature programmed desorption (TPD) experiments. We propose that the coverage dependent adsorption energy can be fit using a functional form including the configurational entropy and linear adsorbate-adsorbate interaction terms. As one example of this scheme, we analyze TPD spectra of CO desorption on Au(211) and Au(310) surfaces. We determine that under atmospheric CO pressure, the *steps* of both facets adsorb between $0.4 - 0.9$ ML coverage of CO*. We show this result to be consistent with density functional theory calculations of adsorption energies with the BEEF-vdW functional.

KEYWORDS: TPD, gold catalysis, CO adsorption, DFT Benchmark

In the past two decades, heterogeneous catalysis has seen tremendous growth in the use of density functional theory (DFT) for mechanistic analysis and computational catalyst discovery.[1] These efforts require accurate descriptions of adsorption energies of key reaction intermediates. DFT functionals have been benchmarked against experiments and, in general, DFT-predicted adsorption energies with workhorse GGA-level functionals are accurate to 0.2 eV.[2] However, benchmark datasets do not typically include noble metals such as gold, which are good catalysts for a variety of thermal and electrochemical catalytic reactions.[3]

Benchmark DFT datasets are generally determined from three experimental techniques: single-crystal adsorption calorimetry (SCAC), equilibrium adsorption isotherms (EAI) and temperature programmed desorption (TPD) experiments.[2–6] SCAC measurements have been shown to be reliable, precise and are an unambiguous way of determining adsorption energies.[7] EAI requires reversible adsorption-desorption but experiments can be fit in a comparatively straightforward manner by using the Clausius-Clapeyron expression.[6] In comparison, TPD provides more features in its output spectra, but requires fitting techniques and interpretation of the underlying kinetics to extract adsorption energies. While TPD requires more analysis than the other two methods, its use is widespread and certain systems relevant to heterogeneous catalysis are characterized only by TPD spectra.[8,9] Thus, simple and precise methods to obtain quantities from TPD to benchmark against computations are valuable.

The central fitting equation for first order desorption TPD spectra is an Arrhenius type relationship, $\text{rate} = \nu(T)\exp\left(-\frac{G_d}{k_B T}\right)\theta$, which relates the rate to an empirical pre-factor, $\nu(T)$, the desorption energy, G_d and the coverage θ. The most commonly used, and simplest method, applies the Redhead equation[10] in its linearized form, $G_d = k_B T_p \ln\left(\frac{\nu T_p}{\beta} - 3.64\right)$, to relate peak(s) in the TPD spectra, T_p, to the adsorption energies on various sites for a given rate of heating, β.

The Redhead equation is derived with the assumption that G_d is independent of coverage and assumes a constant, temperature-independent ν. Alternative techniques, such as Complete Analysis, fit a line to $\ln(\text{rate})$ vs. $1/T$. However, the obtained energies from the analysis have no coverage dependence.[11] A more detailed method was provided by Ref.[12], where a temperature-independent ν and a function $G_d(\theta)$ is fitted to all points from a series of TPD spectra.

In this work, we present a method to extract not just adsorption energies, but also adsorbate-adsorbate interaction parameters and adsorbate saturation coverages directly from fits to TPD spectra. In contrast to other methods, in this approach we explicitly account for a temperature dependent pre-factor and a coverage dependent desorption energy term. The coverage dependence in the adsorption free energy of binding arises from both configurational entropy and linear adsorbate-adsorbate interactions. These effects are relevant at low and high coverages, respectively, and accounting for them allows us to fit the entire TPD peak, even in cases where it overlaps with other peaks. We benchmark the resultant adsorbate-adsorbate interaction parameters against computations. We illustrate the use of this method for reported TPD data for CO adsorbed on Au(211) and Au(310) stepped single crystal facets. We find an adsorption energy of 0.45eV for CO on stepped sites at zero coverage, which differs from that of a Redhead analysis by approximately 0.1 eV. Furthermore, we determine that the equilibrium coverage is between 0.4 to 0.9 ML of CO on step sites. In this particular case, CO binding as a function of coverage is well described by the BEEF-vdW functional.

To illustrate the application of our fitting method, we investigate CO adsorption on Au (211) and Au(310) *steps*. In this system the adsorbate-adsorbate interactions and configurational entropy are particularly important because large CO coverages may be present at the low temperature range of

the TPD, while a very small coverage is expected at the high temperature range. Furthermore, CO binding on metals is a known challenge for DFT due to incorrect alignment of the $2\pi^*$ state.[13] **Figure 1** (a,d) show previously reported CO TPD data on Au(211)[9] and Au(310).[14] Note that in these spectra, we subtracted the baseline signal of CO desorption using an exponential decay function to the tail of this the spectra[15] (see **Figure S1)**. This background signal can arise from, for example, the desorption of CO from the walls of the apparatus.

As **Figure 1**(c,f) illustrate, Au(211) consists of a three-atom-wide (111) *terrace* and a (100) *step*, which we will refer to as the $(111)_{terrace}$ and $(100)_{step}$. Au(310) consists of a three-atom-wide (100) *terrace* and a (110) *step*, which we refer to as $(100)_{terrace}$ and $(110)_{step}$ respectively.

Peak assignments in TPD curves. In **Figure 1**a we assign the peaks at lower temperatures to $(111)_{terrace}$ and higher temperatures to the less coordinated, stronger binding $(100)_{step}$ sites. Similarly, in **Figure 1**d we assign the low temperature peaks to $(100)_{terrace}$ sites, and the high temperature peaks to the $(110)_{step}$.

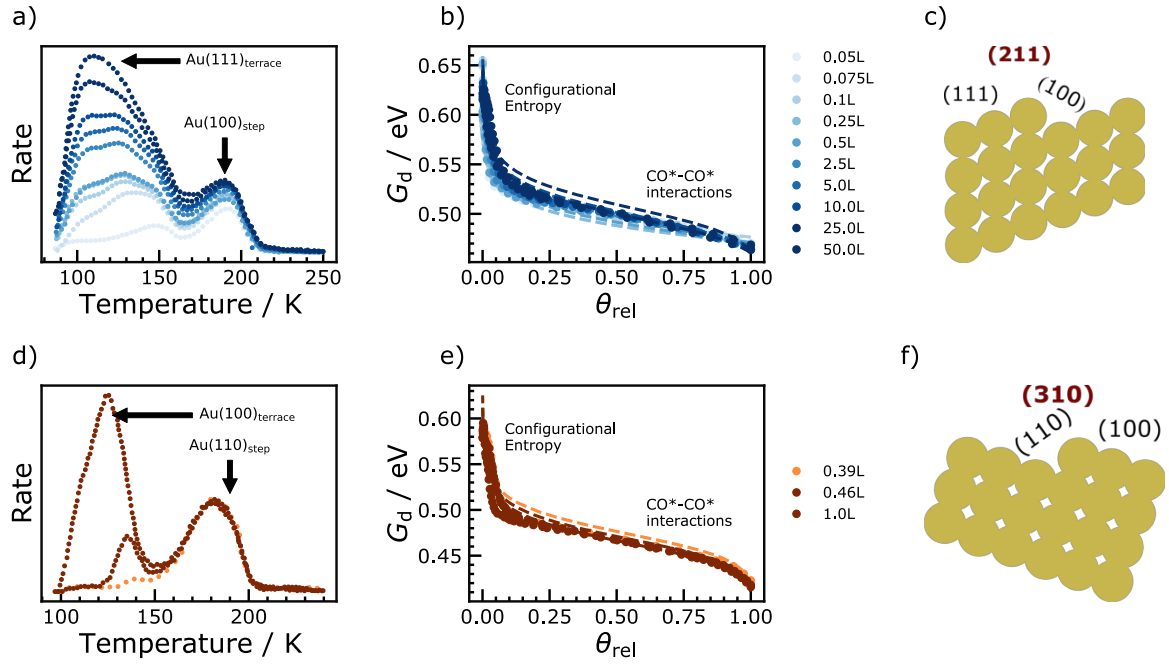

Figure 1: a, d) Background corrected rates of CO desorption from TPD experiments in previous work for Au(211) from Ref[9] and Au(310) Ref.[14] Site motifs assigned to each peak are labelled directly in the figure; b,e) G_d as a function of the relative TPD coverage under vacuum conditions for the $Au(100)_{step}$ and $Au(110)_{step}$; the dashed line indicates the best fit to the points c,f) Schematic of (211) and (310) surfaces.

How to extract adsorption energies and equilibrium coverages from fits of TPD curves. In what follows, we detail how we extract the free energy of CO adsorption, ΔG_{CO^*}, from fitting kinetic parameters to TPD spectra corresponding to different sites. We then translate ΔG_{CO^*} into an equilibrium coverage, on each of these sites under atmospheric pressure and a temperature of 300K.

We assume CO desorption to be a first order kinetic process with no readsorption (i.e. it is irreversible), which has the following rate:

$$\frac{d\theta_{rel}(T)}{dt} = \frac{k_B T}{h} \exp\left(-\frac{G_d(\theta_{rel},T)}{k_b T}\right) \theta_{rel}(T) \qquad (1)$$

where $G_d(\theta_{rel}, T) = G_{\mathrm{CO^{TS}}} - G_{\mathrm{CO^*}}$ is the free energy barrier for CO desorption, and $\theta_{rel}(T)$ is the relative coverage of CO at temperature *T*, obtained by

$$\theta_{rel}(T) = \frac{\int_{Tmin}^{T} \frac{d\theta}{dT} dT}{\int_{Tmin}^{Tmax} \frac{d\theta}{dT} dT} = \frac{\theta}{\theta_{sat}} \quad (2)$$

We obtain *relative* coverages here from TPD spectra, since the coverage determined through integrating under a TPD rate curve provides a value relative to a maximum coverage θ_{sat} for the given initial exposure, $\theta_{rel} = \theta/\theta_{sat}$, where θ is the real coverage in monolayers (ML). Note that here we are considering a temperature-dependent prefactor, $k_B T/h$, from transition state theory,[16] and a coverage-dependent G_d.

By fitting Equation (1) and (2) to the rates in **Figure 1**(a,d) we obtain $G_d(\theta, T)$. **Figure 1**(b,e) shows the resultant G_d vs. θ_{rel} for $(100)_{\mathrm{step}}$ and $(110)_{\mathrm{step}}$ sites, under vacuum conditions (we discuss $(111)_{\mathrm{terrace}}$ and $(100)_{\mathrm{terraces}}$ in **SI Note 1**; briefly, adsorbates on terraces interact with those on step sites, which hinders accurate determination of adsorption energies on terraces from the TPD spectra). At very low coverages, the divergent configurational entropy (detailed below) causes a sharp increase in desorption free energy. As the coverage increases, the binding strength weakens slightly due to adsorbate-adsorbate interactions, which decreases the desorption energy.

The G_d, in terms of of internal energies and entropies, is as follows:

$$G_d = G_{\mathrm{CO^{TS}}} - G_{\mathrm{CO^*}} = (E_{\mathrm{CO^{TS}}} - TS^{\mathrm{harm}}_{\mathrm{CO^{TS}}}) - (E_{\mathrm{CO^*}} + b\theta - TS^{\mathrm{harm}}_{\mathrm{CO^*}}) + \Delta\mathrm{ZPE} - T\Delta S^{\mathrm{config}} \quad (3)$$

where $E_{\mathrm{CO^{TS}}}$ is the internal energy of the surface with CO at the transition state, $E_{\mathrm{CO^*}}$ is the internal energy of the adsorbed state at dilute coverage with $\theta \to 0$, S_x^{harm} the vibrational

contributions to entropy for state *x* as determined using the harmonic approximation, *b* is a CO-CO interaction parameter which accounts for the decrease in desorption energy with increasing θ, $\Delta\mathrm{ZPE}$ and $\Delta S^{\mathrm{config}}$ are the difference in zero point energy and configurational entropy between $\mathrm{CO}^{\mathrm{TS}}$ and CO^{*}, respectively.

In order to obtain $\Delta G_{\mathrm{CO}^{*}}$ from G_d, we assume the following:

1) The internal energy of the transition state ($E_{\mathrm{CO}^{\mathrm{TS}}}$) is well approximated by that of $\mathrm{CO}_{(\mathrm{g})}$, $E_{\mathrm{CO}^{\mathrm{TS}}} \approx E_{\mathrm{CO(g)}} + E_{*}$ (evaluated in **SI Note 2**).

2) The vibrational and rotational entropic contributions associated with the transition state of CO desorption, $S^{\mathrm{harm}}_{\mathrm{CO}^{\mathrm{TS}}}$, are approximated by those of CO*, $S^{\mathrm{harm}}_{\mathrm{CO}^{*}}$, since $\mathrm{CO}^{\mathrm{TS}}$ lies very close to the surface, i.e., $S^{\mathrm{harm}}_{\mathrm{CO}^{\mathrm{TS}}} \approx S^{\mathrm{harm}}_{\mathrm{CO}^{*}}$.

These two assumptions simplify Equation (3) to a function only of *thermodynamic* parameters:

$$G_d \approx E_{\mathrm{CO(g)}} + E_{*} - E_{\mathrm{CO}^{*}} - b\theta + \Delta\mathrm{ZPE} - T\Delta S^{\mathrm{config}} \qquad (4)$$

We define $\Delta E_{\theta\to 0} = E_{\mathrm{CO(g)}} + E_{*} - E_{\mathrm{CO}^{*}} + \Delta\mathrm{ZPE}$, $\Delta E_{\theta\to 0}$ is the desorption energy of CO at the limit of $\theta \to 0$, which is independent of θ. Along with the θ-dependence of $\Delta S^{\mathrm{config}}$, G_d from Equation (4) becomes a function only of θ (the true coverage) or θ_{rel} (the relative coverage) and *T*:

$$G_d(\theta,T) \approx \Delta E_{\theta\to 0} - b\theta - k_b T\ln\left(\frac{\theta}{1-\theta}\right) = \Delta E_{\theta\to 0} - b\theta_{rel}\theta_{sat} - k_b T\ln\left(\frac{\theta_{rel}\theta_{sat}}{1-\theta_{rel}\theta_{sat}}\right) \qquad (5)$$

We apply the righthand side of Equation (5) to fit the curves in **Figure 1**(b,e)**.** The resultant $\Delta E_{\theta\to 0}$ are shown in **Figure 2**a as a function of initial exposures. Within error bounds, $\Delta E_{\theta\to 0}$

does not vary with exposure, which is consistent with $\Delta E_{\theta\to 0}$ having no dependence on coverage. The other two contributions to $G_d(\theta, T)$ are shown in **Figure 1**b. The configurational entropy term shows a large contribution only at very low coverages, while the interaction term contributes at higher coverages. The fit parameters, b and θ_{sat}, are tabulated in **SI Note 3**.

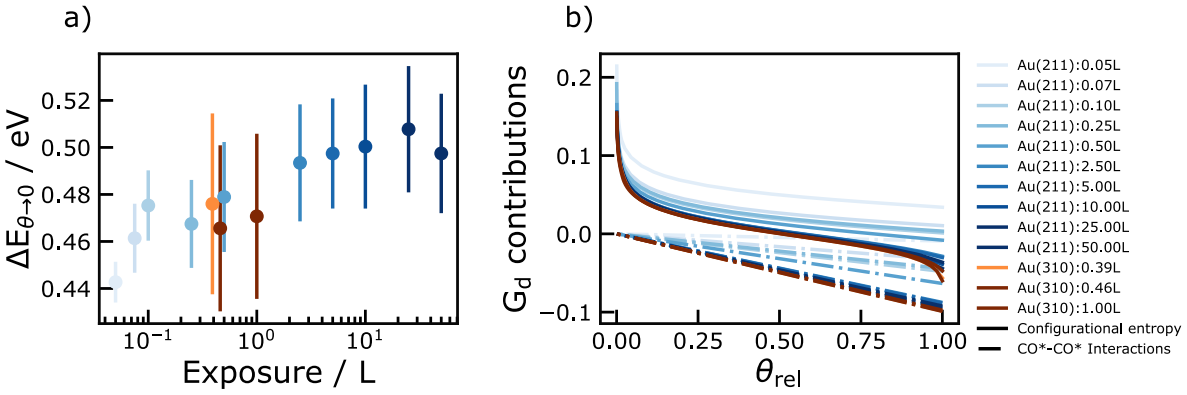

Figure 2: a) Desorption energy corresponding to dilute coverages, $\Delta E_{\theta\to 0}$ of CO for $(100)_{step}$ and $(110)_{step}$ as a function of the initial exposure in Langmuir in the TPD experiment. Error bars show errors from the fit determined as the mean error of the residual; b) Contributions of the configurational entropy (solid lines) and CO-CO adsorbate-adsorbate interaction (dashed-lines) to the total desorption energy G_d based on the fitting equation described in Equation 5.

To obtain the *equilibrium* $\theta(T, p_{\mathrm{CO}})$, we translate $G_d(\theta, T)$ into the *free energy of adsorption*, $\Delta G_{\mathrm{CO}^*}(\theta, T)$, by adding the *difference* in the entropic contributions arising from CO*, $S^{\mathrm{harm}}_{\mathrm{CO}^*}$, and $\mathrm{CO}_{(g)}$, $S^{\mathrm{ideal}}_{\mathrm{CO(g)}}$, as well as the pressure of $\mathrm{CO}_{(g)}$, p_{CO}:

$$\Delta G_{\mathrm{CO}^*}(\theta, T) \approx -G_d(\theta, T) - T\left(S^{\mathrm{harm}}_{\mathrm{CO}^*} - S^{\mathrm{ideal}}_{\mathrm{CO(g)}}\right) - k_b T \ln(p_{\mathrm{co}}) \qquad (6)$$

We obtain $S^{\mathrm{harm}}_{\mathrm{CO}^*}$ and $S^{\mathrm{ideal}}_{\mathrm{CO(g)}}$ with calculations of vibrational frequencies from DFT (tabulated in the **Table S1**). Combining Equations (5) and (6), we obtain $\Delta G_{\mathrm{CO}^*}(\theta, T)$ in terms of fitted parameters from $G_d(\theta, T)$:

$$\Delta G_{\mathrm{CO}^*}(\theta,T) \approx -\Delta E_{\theta\to 0} + b\theta + k_b T\ln\left(\frac{\theta}{1-\theta}\right) - T\left(S^{\mathrm{harm}}_{\mathrm{CO}^*} - S^{\mathrm{ideal}}_{\mathrm{CO(g)}}\right) - k_b T\ln(p_{\mathrm{co}}) \qquad (7)$$

We solve Equation (7) numerically for the *equilibrium* $\theta(T)$, under the equilibrium condition $\Delta G_{\mathrm{CO}^*}(\theta,T) = 0$. **Figure 3** shows the equilibrium $\theta(T)$ for $p_{CO(g)} = 1$ bar as a function of T for all exposures. Given that 1ML (monolayer) corresponds to complete coverage of sites, all exposures on both $(100)_{\mathrm{step}}$ and $(110)_{\mathrm{step}}$ sites show approximately a coverage of between 0.4 to 0.9 ML present on both (211) and (110) surfaces at a temperature of 300 K and pressure of 1 bar $\mathrm{CO}_{(g)}$.

As a side note: the $\Delta G_{\mathrm{CO}^*}(\theta,T) = 0$ condition gives rise to a physically intuitive adsorption isotherm expression.[17] At standard conditions, $\theta = \frac{1}{2}$ and $p_{\mathrm{co}} = 1\mathrm{bar}$, we define a= $\Delta G_{\theta=\frac{1}{2}} = -\Delta E_{\theta\to 0} + \frac{b}{2} - T\left(S^{\mathrm{harm}}_{\mathrm{CO}^*} - \mathrm{S}^{\mathrm{total}}_{\mathrm{CO(g)}}\right)$ and write Equation (7) in terms of $\Delta G_{\theta=\frac{1}{2}}$

$$\Delta G_{\mathrm{CO}^*}(\theta,T) = \Delta G_{\theta=\frac{1}{2}} + b\left(\theta - \frac{1}{2}\right) + k_b T\ln\left(\frac{\theta}{1-\theta}\right) - k_b T\ln(p_{\mathrm{co}}) \qquad (8)$$

With $\Delta G_{\mathrm{CO}^*}(\theta,T) = 0$ in Equation (8), the equilibrium θ can be expressed implicitly in terms of the equilibrium constant, $K(\theta,T)$, in the form of an adsorption isotherm:

$$\theta(T,p_{\mathrm{CO}}) = \frac{K_{(\theta,T)}p_{\mathrm{CO}}}{1 + K_{(\theta,T)}p_{\mathrm{CO}}}, \quad K(\theta,T) = \exp\left(-\frac{\Delta G_{\theta=\frac{1}{2}} + b\left(\theta - \frac{1}{2}\right)}{k_b T}\right) \qquad (9)$$

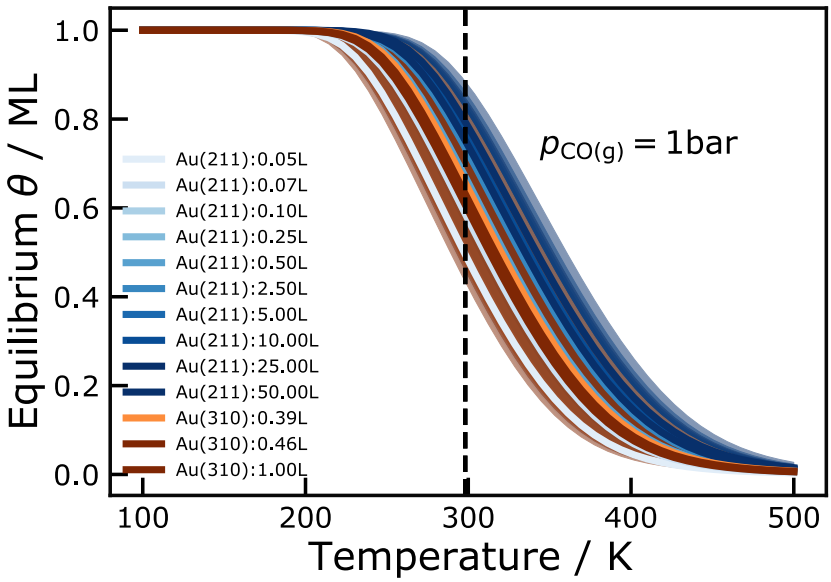

Figure 3: Equilibrium coverage of CO as a function of the temperature at 1 bar $CO_{(g)}$ pressure for both surface facets (211) and (310) for all considered initial exposures. The dashed black line shows the equilibrium coverage at 298.15K.

Comparison of TPD-derived and DFT adsorption energies. We evaluate the $\Delta E_{\theta\to 0}$ and equilibrium θ from TPD against GGA-DFT calculations of adsorbed CO on periodic Au(111), Au(100) terraces and Au(110), Au(211), Au(310) stepped facets (see **SI Note 2**). By varying the number of CO* within the periodic unit cells in our simulations, we calculate two quantities – 1) $\Delta E + \Delta\mathrm{ZPE}$, which can be directly compared with $\Delta E_{\theta\to 0}$ 2) ΔG_{diff}, the *differential* CO adsorption free energy at various coverages:

$$\Delta G_{\mathrm{diff}} = \frac{G_{m_{\mathrm{CO}^*}} - G_{n_{\mathrm{CO}^*}} - (m_{CO} - n_{CO})G_{\mathrm{CO}_{(g)}}}{m_{\mathrm{CO}} - n_{\mathrm{CO}}}, \qquad (10)$$

where $G_{x_{\mathrm{CO}}}$ is the free energy corresponding to a state with x adsorbed CO* and $G_{\mathrm{CO}_{(g)}}$ is the free energy of $CO_{(g)}$. Analogous to how to was defined for the TPD experiment in Equation (2), we

define the coverage θ as the number of CO* per surface atom for the (111), (100), and (110) facets and per step atom for the (211) and (310) facet. We report both $\Delta E + \Delta\mathrm{ZPE}$ and ΔG_{diff} as a function of θ in **Figure 4** for all facets considered; overall, we see the increase in ΔG_{diff} with increasing θ, which arises from increasing adsorbate-adsorbate interactions. An exception is (310), where the energies stay constant. We attribute this behavior to a larger spacing between the step sites in (310) as compared to (211), reducing adsorbate-adsorbate interactions. In the case of (211), we attribute the slight dip at low θ to slight restructuring of the surface upon adsorption of CO*.

We indicate the $\Delta E_{\theta\to 0}$ obtained from TPD for $(100)_{\mathrm{step}}$ and $(110)_{\mathrm{step}}$ facets in **Figure 4**a by the light blue and red bands (the width indicates the uncertainty arising from fits to different exposures). Within error bounds, the difference between the computational $\Delta E + \Delta\mathrm{ZPE}$ at the lowest coverages evaluated compared to TPD-derived $\Delta E_{\theta\to 0}$ is less than 0.1 eV in the weaker binding direction for the (211) and (310) steps. In comparison, the Redhead analysis (see **SI Note 1**), gives a $\Delta E_{\theta\to 0} = 0.58$ eV, which differs from $\Delta E + \Delta\mathrm{ZPE}$ obtained from our analysis by 0.1 eV in the stronger binding direction.

We also determine a GGA-DFT predicted equilibrium θ from the data in **Figure 4**b**.** The equilibrium θ is reached where the differential *free* energy of adsorption is zero:

$$\Delta G_{diff} = 0, \qquad (11)$$

and is shown in **Figure 4**b as a black line. The free energy includes the entropy of gas phase and adsorbed CO as well as its configurational entropy. The computed equilibrium θ is therefore up to 0.3 ML on the (211) and 1ML on (310) stepped facets while no coverage of CO is likely on (111) and (100) terraces.

Overall, the energies obtained from the above TPD analysis and the DFT calculations both suggest that CO binds to the *step* sites of Au (211) and (310)/(110) at standard temperature, 298.15 K and pressure of 1 bar $CO_{(g)}$. ΔG_{CO^*} obtained from TPD (given by Equation 5) and the BEEF-vdW functional deviate by about 0.1eV, which gave rise to the differences in predicted equilibrium θ. Overall, we find that the BEEF-vdW functional accurately predicts the adsorption energies accurately as compared to the TPD extracted values.

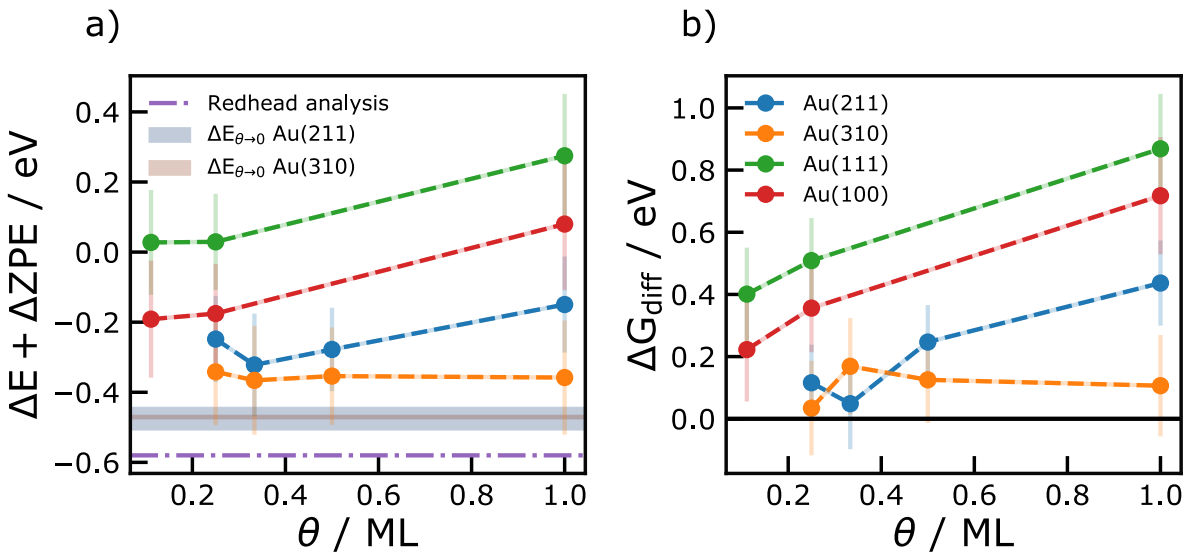

Figure 4: DFT calculated a) adsorption energies b) differential free energies for CO adsorption at different coverages for the most stable adsorption site; in a) the colored bands indicate $\Delta E_{\theta \to 0}$ obtained from the TPD analysis for each facet, and the purple dashed line the value from Redhead analysis.

Conclusions

CO adsorption on Au(211) and Au(310) surfaces are investigated using TPD and DFT calculations. We establish a simple methodology to extract adsorption energies and equilibrium coverages using

TPD spectra and benchmark the obtained values with DFT calculations. The approach involves fitting the desorption energy from experimental TPD spectra to a functional form that includes the adsorption energy as a function of the entire range in coverage, through the configurational entropy and a linear adsorbate-adsorbate interaction term. This treatment is in contrast to the Redhead analysis which assumes coverage independent adsorption energies. We find under standard conditions with 1 bar CO and 298.15 K, $0.4 - 0.9$ ML of CO may be present on the Au steps. Furthermore, we show that for Au step sites, computed adsorption energy and equilibrium coverages from the BEEF-vdw functional are in good agreement with TPD extracted values.

Computational Methods

Density functional theory calculations were performed using Vienna Ab-initio Software Package (VASP).[18] Core electrons were described using Projector Augmented Waves (PAW)[19] potentials. Valence electrons were described using plane-waves with kinetic energy up to 500eV for static calculations. Gaussian smearing with a width of 0.1eV was used. The BEEF-vdW[4] functional was used for all calculations. All calculations were run without spin-polarization.

Structures were prepared using the Atomic Simulation Environment (ASE)[20]. The lattice constant of gold was optimized using a 12x12x12 Monkhorst-Pack[21] *k*-point mesh grid and was determined to be 4.205Å. Slabs four layers thick were made for (111), (100), (110) and (211) facets were constructed, with the bottom two layers kept fixed. For the (100) and (111) surfaces (1x1), (2x2), and (3x3) cells were used with *k*-points (12,12,1), (6,6,1) and (4,4,1) respectively. For the (211) surface, (1x3), (2x3), (3x3) and (4x3) cells were used with *k*-points (12,4,1),

(6,4,1), (4,4,1) and (3,4,1) respectively. For the (310) surface (1x4), (2x4), (3x4) and (4x4) cells were used with *k*-points (12,6,1), (6,6,1), (4,6,1) and (3,6,1) respectively.

Static adsorption energies for CO were calculated on all unique surface sites on each facet. Initial adsorbate geometries were generated using CatKit.[22] All geometries were optimized until forces on all atoms was less than $0.025\text{eV}\text{Å}^{-1}$. Vibrational frequencies were computed using a finite difference method as implemented in VASP ($IBRION = 5$) and calculated only for the surface adsorbate.

Code availability

Python code to fit TPD spectra is available on https://www.fysik.dtu.dk/english/research/cattheory/electro-catalysis/software upon publication

Acknowledgements

Funding from the Villum Fonden through the VSUSTAIN project (9455) is gratefully acknowledged. The authors thank Jens K. Nørskov for the discussion regarding TPD spectra. YK would like to acknowledge financial support from the Japan Society for the Promotion of Science (JSPS) KAKENHI Grant-in-Aid for Early-Career Scientists (19 K15360) and JSPS Open Partnership Joint Research Projects/Seminars (JPJSBP 120209925).

References

1. Nørskov, J. K., Bligaard, T., Rossmeisl, J. & Christensen, C. H. Towards the computational design of solid catalysts. *Nat. Chem.* **1**, 37–46 (2009).

2. Mallikarjun Sharada, S., Karlsson, R. K. B., Maimaiti, Y., Voss, J. & Bligaard, T. Adsorption on transition metal surfaces: Transferability and accuracy of DFT using the ADS41 dataset. *Phys. Rev. B* **100**, 35439 (2019).

3. Wellendorff, J. *et al.* A benchmark database for adsorption bond energies to transition metal surfaces and comparison to selected DFT functionals. *Surf. Sci.* **640**, 36–44 (2015).

4. Wellendorff, J. *et al.* Density functionals for surface science: Exchange-correlation model development with Bayesian error estimation. *Phys. Rev. B - Condens. Matter Mater. Phys.* **85**, 235149 (2012).

5. Bligaard, T. *et al.* Toward Benchmarking in Catalysis Science: Best Practices, Challenges, and Opportunities. *ACS Catalysis* **6**, 2590–2602 (2016).

6. Campbell, C. T. & Sellers, J. R. V. Enthalpies and entropies of adsorption on well-defined oxide surfaces: Experimental measurements. *Chemical Reviews* **113**, 4106–4135 (2013).

7. Campbell, C. T. Energies of Adsorbed Catalytic Intermediates on Transition Metal Surfaces: Calorimetric Measurements and Benchmarks for Theory. *Acc. Chem. Res.* **52**, 984–993 (2019).

8. Van Reijzen, M. E., Van Spronsen, M. A., Docter, J. C. & Juurlink, L. B. F. CO and H2O adsorption and reaction on Au(310). *Surf. Sci.* **605**, 1726–1731 (2011).

9. Kim, J., Samano, E. & Koel, B. E. CO adsorption and reaction on clean and oxygen-covered Au(211) surfaces. *J. Phys. Chem. B* **110**, 17512–17517 (2006).

10. Division, E. E. Thermal desorption of gases. *Vacuum* **12**, 274 (1962).

11. de Jong, A. M. & Niemantsverdriet, J. W. Thermal Desorption Analysis: Comparative Test of Ten Commonly Applied Procedures. *Surf. Sci.* **233**, 355–365 (1990).

12. Tait, S. L., Dohnálek, Z., Campbell, C. T. & Kay, B. D. N-alkanes on MgO(100). I. Coverage-dependent desorption kinetics of n-butane. *J. Chem. Phys.* **122**, (2005).

13. Feibelman, P. J. *et al.* The CO/Pt(111) Puzzle †. *J. Phys. Chem. B* **105**, 4018–4025 (2002).

14. Weststrate, C. J. *et al.* CO adsorption on Au(3 1 0) and Au(3 2 1): 6-Fold coordinated gold atoms. *Surf. Sci.* **603**, 2152–2157 (2009).

15. Chorkendorff, I. & Tougaard, S. Background subtraction in electron spectroscopy by use of reflection electron energy loss spectra. *Appl. Surf. Sci.* **29**, 101–112 (1987).

16. Nørskov, J. K., Studt, F., Abild-Pedersen, F. & Bligaard, T. *Fundamental Concepts in Heterogeneous Catalysis*. *Fundamental Concepts in Heterogeneous Catalysis* **9781118888**, (Wiley Blackwell, 2014).

17. Pursell, C. J., Hartshorn, H., Ward, T., Chandler, B. D. & Boccuzzi, F. Application of the Temkin model to the adsorption of CO on gold. *J. Phys. Chem. C* **115**, 23880–23892 (2011).

18. Kresse, G. & Furthmüller, J. Efficient iterative schemes for ab initio total-energy calculations using a plane-wave basis set. *Phys. Rev. B - Condens. Matter Mater. Phys.* **54**, 11169–11186 (1996).

19. Joubert, D. From Ultrasoft Pseudopotentials to the Projector Augmented-wave Method. *Phys. Rev. B - Condens. Matter Mater. Phys.* **59**, 1758–1775 (1999).

20. Hjorth Larsen, A. *et al.* The Atomic Simulation Environment - A Python Library for Working with Atoms. *J. Phys. Condens. Matter* **29**, 30 (2017).

21. Monkhorst, H. J. & Pack, J. D. Special Points for Brillouin-zone Integrations. *Phys. Rev. B* **13**, 5188–5192 (1976).

22. Boes, J. R., Mamun, O., Winther, K. & Bligaard, T. Graph Theory Approach to High-Throughput Surface Adsorption Structure Generation. *J. Phys. Chem. A* **123**, 2281–2285 (2019).